Rationalization of Noncovalent Interactions within Six New MII/8-Aminoquinoline Supramolecular Complexes (MII = Mn, Cu, and Cd): A Combined Experimental and Theoretical DFT Study

Masoud Mirzaei,Hossein Eshtiagh-Hosseini, Zahra Bolouri, Zahra Rahmati, Atefeh Esmaeilzadeh, Azam Hassanpoor, Antonio Bauza, Pablo Ballester, Miquel Barceló-Oliver, Joel T. Mague, Behrouz Notash, and Antonio Frontera,

ABSTRACT: To examine the influence of the metal ions and their counterions on crystalline networks, we have designed and synthesized six MX2/8-aminoquinoline (8-aq) (M = MnII, CuII,
CdII and X = Cl−, Br−, I−, NO3 −, SCN−) complexes, having the formulas [Mn(8-aq)2 I2]·(1), [Mn(8-aq)2(H2O)2](8-aq)3·Br2 (2), [Mn(8-aq)2(SCN)2] (3), [Cu(8-aq)2Cl(H2O)]·Cl·H2O (4), [Cu(8-aq)2(NO3)(H2O)]·NO3 (5), and Cd(8-aq)2I2 (6). Single-crystal Xray diffraction analyses showed that all of the complexes have a distorted octahedral geometry, in which each 8-aq molecule acts as a bidentate ligand and coordinates to the central metal ion with its common coordination mode, to form an N,N′ chelating motif.
Remarkably, the influence of the counterion on the geometry of the complex is very significant since both I− and SCN− anions are coordinated to the metal ion in compounds 1, 3, and 6, adopting a cis configuration, while a single anion occupies an axial position in compounds 4 and 5 (Cl− and NO3−, respectively) and the other counterion is not coordinated. Finally, both Br− anions are not coordinated in the cationic complex 2 (Mn metal center). In all cases, there are extended supramolecular networks due to cooperativity hydrogen-bonding and π−π stacking interactions that play an essential role in the formation and stability of the crystalline materials. The binding energies attributed to the different interactions have been evaluated using DFT calculations.

1. INTRODUCTION

In modern terminology, the meaning of “supramolecular” has become closely related to a strategy to control self-assemblies, tightly linked to coordinative interactions between metals and organic ligands, which also interact through intermolecular forces, such as hydrogen-bonding, donor−acceptor, and π−π stacking interactions.1 In crystal engineering, some powerful synthetic factors for controlling the self-assembly process and the construction of desired supramolecular architectures with potential applications2−4 are at hand, such as the nature of the metal center5−8 and its counterions,9−11 steric and conformational properties of the organic ligand,12,13 and the reaction conditions.14−17 A common feature of such design approaches is the use of polyfunctional organic ligands as geometrically predetermined units, and metal salts containing various counterions with a different ability to coordinate.17Several independent systematic studies involving MX2/N-heterocyclic ligands (M = Zn, Cd, Hg, Ag, Cu, and Fe; X = NO3, SCN, Cl,
Br, I, SO4)18−29 are available in the literature devoted to explore possible correlations between these factors with structuralparameters, geometries, and the self-assembly pattern in crystalline networks. Some of us have also investigated the self-assembly process of organic/inorganic motifs into a crystalline network using 8-aq as organic ligand and mercury halides to rationalize the impact of the counter-halides on the solid-state architecture.21Ligand 8-aq and its derivatives have recently attracted attention because of their antiprotozoal and other medicinal properties.19 As a ligand, 8-aq is a relatively bulky chelating planar ligand with excellent features that make it extremely interesting in supramolecular chemistry: (1) Its NH2 functional group can coordinate to a metal, but it can also participate in hydrogen-bonding interactions. (2) It can provide π−π stacking interactions with aromatic rings, thus controlling the intergrowth of interpenetrating networks.30−32 As a continuation of our efforts to investigate the influence of the metal ion and its accompanying anions on the resulting 8-aq complexes, we have designed and synthesized six coordination compounds [Mn(8-aq)2I2] (1), [Mn(8-aq)2(H2O)2](8-aq)2· Br2 (2), [Mn(8-aq)2(SCN)2] (3), [Cu(8-aq)2Cl(H2O)]Cl·H2O (4), [Cu(8-aq)2(NO3)(H2O)]·NO3 (5), and [Cd(8-aq)2I2] (6) by utilizing different manganese, copper, and cadmium salts containing Cl−, Br−, I−, NO3−, and SCN− anions (see Scheme 1). They have been characterized by elemental analyses and IR spectroscopy and have been structurally determined by singlecrystal X-ray diffraction analysis. The X-ray crystallography studies demonstrate that π−π stacking and hydrogen-bonding interactions are crucial to the formation and generation of various higher-dimensional (3D) networks. In addition, we have analyzed energetically these π−π and H-bonding interactions by means of DFT calculations.

Scheme 1.

2. EXPERIMENTAL SECTION

2.1. Materials and Instrumentation. All reagents and solvents were purchased from commercial sources and were used directly without further purification. Infrared spectra in the range of 4000−600cm−1 were recorded on a Buck 500 scientific spectrometer using KBr discs. Elemental analyses were carried out with a Thermo Finnigan Flash-1112EA microanalyzer and PerkinElmer 2004(II) apparatus. For the structures of 1−6, X-ray data were obtained with a Bruker APEX II CCD diffractometer. Melting points were determined on a Barnstead Electrothermal 9300 apparatus.

2.1.1. X-ray Crystallography. For 1−6, the crystals were mounted on a glass fiber and flash-frozen to 100−150 K (Oxford Cryosystems- Cryostream cooler). A preliminary examination and intensity data collection were carried out using an APEX II CCD diffractometer, ω scans, and graphite-monochromated Mo−Kα radiation generated from an X-ray tube operating at 50 kV and 25 mA. The data were corrected for Lorentz and polarization effects (see Table 1). The images were interpreted and integrated with the program CrysAlisPro.33 All structures were solved by direct methods (SHELXS97)34 and refined by the full-matrix least-squares method on all F2 data (SHELXL97).35
2.1.2. Computational Methods. The energies of all complexes included in this study were computed at the BP86-D3/def2-TZVP level of theory. The geometries have been obtained from the crystallographic coordinates. The calculations have been performed by using the program TURBOMOLE version 6.5.36 The interaction energies were calculated with correction for the basis set superposition error (BSSE) by using the Boys−Bernardi counterpoise technique.37 For the calculations, we have used the BP86 functional with the latest available correction for dispersion (D3). For the ligand-exchange study, we have optimized the complexes imposing either C2h or Ci symmetry constrain for the Cu(8-aq)2X2 and [Cu(8-aq)2(H2O)2]X2 complexes, respectively.
2.2. Synthesis of [Mn(8-aq)2I2] (1). A saturated solution (5 mL) of sodium iodide was added to an aqueous solution (5 mL) of Mn(CH3COO)2·4H2O (24 mg, 0.10 mmol). A 50 mg (0.35 mmol) portion of 8-aminoquinoline (8-aq) in 5 mL of MeOH was added dropwise to the previous solution, and the mixture was stirred for 1 h at room temperature. By slow evaporation of the solvent, green plate single crystals of 1 were obtained after 5 days. Yield: 56% (based on Mn). IR (KBr pellet, cm−1): 3196, 3095 (N-H); 1504, 1469 (C□C); 1372 (C□N); 1006 (C-N). Anal. Calcd for C18H16I2MnN4: C, 36.2; H, 2.34; N, 9.38. Found: C, 36.1; H, 2.28; N, 9.33% . mp 270 °C.
2.3. Synthesis of [Mn(8-aq)2(H2O)2](8-aq)3·Br2 (2). The preparation of 2 is similar to that of 1, except that NaBr was used instead of NaI. Pale yellow block crystals of 2 were obtained after 5 days. Yield: 45% (based on Mn). IR (KBr pellet, cm−1): 3307 (O-H); 3163, 3090 (N-H); 1509 (C□C); 1371 (C□N); 1080(C-N). Anal. Calcd for C45H44Br2MnN10O2: C, 52.38; H,4.15; N,13.57. Found: C, 52.35; H, 4.12; N,13.50%. mp 220 °C.
2.4. Synthesis of [Mn(8-aq)2(SCN)2] (3). A mixture of 8-aq (43mg, 0.30 mmol) and KSCN (29 mg, 0.30 mmol) in 10 mL of methanol was added to 10 mL of a methanolic solution of MnCl2· 2H2O. The pale brown solution was stirred for 1 h. By slow evaporation of the solvent at room temperature, pale yellow block single crystals of 3 were obtained after 1 week. Yield: 67% (based on Mn). IR (KBr pellet, cm−1): 3202, 3110 (N-H); 2076 (C-N)SCN −; 1503, 1471 (C□C); 1395 (C□N); 1008 (C-N). Anal. Calcd for C20H16MnN6S2: C, 52.27; H, 3.04; N, 18.29; S, 13.95. Found: C, 52.38; H, 3.09; N, 18.35; S, 13.88%. mp 240 °C.
2.5. Synthesis of [Cu(8-aq)2Cl(H2O)]Cl·H2O (4). A 50 mg (0.34 mmol) portion of 8-aq in 7 mL of MeOH was added dropwise to a clear solution of 60 mg of (0.34 mmol) CuCl2·2H2O in a mixture of methanol (2 mL) and water (5 mL). It was stirred for 2 h. By slow evaporation of the solvent at room temperature, black block single crystals of 4 were obtained. Yield: 80% (based on Cu). IR (KBr pellet, cm−1): 3354 (O-H); 3230, 3155 (N-H); 1505, 1476 (C□C); 1385 (C□N); 896 (C-N). Anal. Calcd for C18H20Cl2CuN4O2: C, 47.28; H, 3.94; N, 12.26. Found: C, 47.25; H, 3.91; N, 12.25%. mp 220 °C.
2.6. Synthesis of [Cu(8-aq)2(NO3)(H2O)]·NO3 (5). The preparation of 5 is similar to that of 4, except that CuCl2·2H2O was replaced by Cu(NO3)2·3H2O (83 mg, 0.34 mmol). Black plate crystals of [Cu(8 aq)2(NO3)(H2O)]·NO3 were obtained after 1 week. Yield: 78% (based on Cu). IR (KBr pellet, cm−1): 3405 (O-H); 3218, 3177 (NH); 1514 (C□C); 1374, 1100 (NO3); 906 (C-N). Anal. Calcd for C18H18CuN6O7: C, 43.91; H, 3.25; N, 17.07. Found: C, 43.83; H, 3.19; N, 17.05%. mp 230 °C.
2.7. Synthesis of [Cd(8-aq)2I2] (6). A 40 mg (0.27 mmol) portion of 8-aminoquinoline (8-aq) in 5 mL of MeOH was added dropwise to an aqueous solution (5 mL) of CdI2 (50 mg, 0.13 mmol). The colorless solution was stirred for 2 h at room temperature. Pale yellow block crystals were obtained by slow evaporation of the solution after 2 weeks. Yield: 51% (based on Cd). IR (KBr pellet, cm−1): 3290, 3214 (N-H); 1576 (C□C); 1499 (C□N); 988 (C-N). Anal. Calcd for C18H16CdI2N4: C, 33.10; H, 2.14; N, 8.58. Found: C, 33.08; H, 2.16; N, 8.55%. mp 200 °C.+

Table 1.

3. RESULTS AND DISCUSSION

3.1. IR Spectra. All compounds show a moderately sharp absorption in the 3090−3290 cm−1 range, which is attributed to the asymmetric stretching of coordinated NH2. The presence of medium intense broad bands in the 3307−3405 cm−1 region is related to the coordinated H2O in complexes 2, 4, and 5. Also, bands at 2079 and 1100 cm−1 are evidence of the existence of coordinated SCN− and NO3 − anions in 3 and 5, respectively.38 These findings are supported by the solid-state structures obtained from X-ray diffraction measurements.
3.2. Description of the Crystal Structures. The crystallographic data for compounds 1−6 are shown in Table 1, while selected bond lengths and bond angles are given in Table 2. Hydrogen bond geometries of the six compounds are shown in Table 3.
3.2.1. [Mn(8-aq)2I2] (1). The X-ray crystal structure analysis reveals that the asymmetric unit of 1 contains one MnII ion, one 8-aq ligand, and one coordinated I− counteranion. As shown in Figure1A, the MnII ion is six coordinated and has a distorted octahedral coordination configuration composed of two amino and two aromatic N atoms from two different 8-aq ligands and two terminal iodide anions (the Mn−N distances range from 2.231 to 2.318 Å, and Mn−I distance is 2.9125 Å). In 1, two bidentate chelating 8-aq are almost perpendicular (N2i−Mn1−N1, 95.36(16)°) with the dihedral angle 46.63(6)° and disposed in a cis configuration. Moreover, two adjacent neutral complexes are linked via N1−H1A···I1 (N/I distance 3.822(5) Å) hydrogen bonds involving I− counterions and 8-aq

fragments to generate an array with the ring having the graph-set notation R2 2(8); see Figure 2A. These dimeric units are further organized into an infinite one-dimensional chain through π−π stacking interactions (centroid-to-centroid distances Cg1···Cg1 = 3.564 Å and Cg1···Cg2 = 3.552 Å running along the c axis (Figure 2B). Both hydrogen bond and π-stacking interactions lead to the formation of a onedimensional supramolecular architecture and play a substantial role in the stabilization of crystal lattice. The energetic features of the dimers and the π-stacking binding mode observed in the solid state are further analyzed below in the theoretical study.

3.2.2. [Mn(8-aq)2(H2O)2](8-aq)3·Br2 (2). The molecular structure of 2 consists of one cationic complex [Mn(8-aq)2(H2O)2]2+, three neutral 8-aq moieties, and two Br− counterions. The MnII ion is located in the basal plane of an elongated octahedron and is coordinated by two 8-aq molecules that lie on the equatorial plane and chelate to the Mn metal center via two amino and two ring N atoms (The Mn−N distances 2.241(2), 2.244(3) Å), while the axial positions are occupied by two oxygen atoms from aqua ligands (Mn−O, 2.216(3) Å) (see Figure 1B).The Br− counteranions occupy the void space between mononuclear complexes and cocrystallized free 8-aq ligands, participating in four N−H···Br hydrogenbonding interactions, two with the free 8-aq ligands and two with the mononuclear complexes (see Figure S1, Supporting Information). Moreover, the Br− anion also establishes an O− H···Br (O/Br distance 3.216(3) Å) hydrogen bond with the coordinated water molecule. The uncoordinated 8-aq ligand also interacts with the coordinated water molecule by means of a N−H···OW hydrogen bond. This hydrogen-bonding network is responsible for the formation of the ab plane of the crystal structure of 2. In addition, coordinated and uncoordinated ligands participate in π−π stacking interactions: centroid-tocentroid distances (Å) 3.721 (Cg1···Cg2), 3.639 (Cg3···Cg4), and 3.737 (Cg3···Cg5) (see Figure 3).

3.2.3. [Mn(8-aq)2(SCN)2] (3). In complex 3, the asymmetric unit contains one Mn atom, two 8-aq molecules as bidentate chelating ligands, and two monodentate SCN− anions as coligands (see Figure 1C). The distorted octahedral coordination sphere around the MnII ion is formed by six nitrogen atoms, four of them belonging to two different 8-aq molecules (Mn−N1, 2.2572(15) Å, Mn−N2, 2.2977(15) Å, Mn−N3, 2.2557(15) Å, Mn−N4, 2.3062(15) Å) and the other two being supplied by two SCN− anions (Mn−N5, 2.1870(17) Å, Mn− N6, 2.1847(18) Å). The SCN− anions occupy cis positions with a N5−Mn−N6 of 86.85(6)° angle, while the two 8-aq units are almost perpendicular to each other. This structural arrangement is stabilized by some intermolecular interactions such as N− H···S (N/S distances range from 3.3121(16) to 3.5161(16) Å) and C−H···S (C/S distances 3.7489(19), 3.827(2) Å) hydrogen bonds involving the SCN− anions and 8-aq moieties (Figure 4A) from neighboring molecular units that generate zigzag assemblies along the b axis. These zigzag strands are packed through π−π stacking interactions between 8-aq aromatic rings with a π−π distance of Cg1···Cg2 = 3.716 Å, to form an infinite 1D chain (Figure 4B).

3.2.4. [Cu(8-aq)2Cl(H2O)]Cl·H2O (4). The asymmetric unit of 4 is composed of one cationic complex, [Cu(8-aq)2Cl (H2O)]+, one Cl− anion, and one lattice water molecule (Figure 1D). In the cationic complex, each copper atom is located at the center of an elongated octahedron as a result of a pronounced Jahn− Teller effect. The equatorial plane around the CuII ion consists of two ring N atoms (Cu−N2, 2.020(4) Å and Cu−N4, 1.999(5) Å) and two amino N atoms (Cu−N1, 1.989(5) Å and Cu−N3, 2.000(5) Å) from two neutral 8-aq ligands that are coordinated in a “head-to-tail” fashion. The N1−Cu−N2 and N3−Cu−N4 angles are 84.00(2)° and 84.10(2)°, respectively, as a result of the “short bite” of the 8-aq ligands. The axial positions are occupied by the O atom of an aqua ligand (Cu−O1, 2.593(4) Å) and a Cl atom (Cu−Cl, 2.825(1) Å). The halogen atom interacts simultaneously with the metal cation and a neighboring NH2 group to form a N−H···Cl hydrogen bond. The driving force for the assembly of this crystal structure is the presence of extensive N−H···Cl and O−H···Cl (N/Cl and O/Cl distances 3.285(5), 3.233(4) Å) hydrogen bonding between the coordinated Cl, aqua and amino group of 8-aq that joins discrete cationic complexes to create infinite 1D chains along the crystallographic b axis. Two neighboring 1D chains connect to each other by π−π stacking interactions (centroid-to-centroid distance is Cg1···Cg2 = 3.560 Å) through the 8-aq aromatic rings in an antiparallel fashion. Furthermore, the lattice water molecules and chloride ions are accommodated in the ab plane,

Table 2.

Table 3.

Figure 1.

Figure 2.

Figure 3.

Figure 4.

forming hydrogen bonds with the 1D chains and with other lattice water molecules, generating a 2D supramolecular network (see Figure 5).

Figure 5.

Table 4.

Figure 6.

3.2.5. [Cu(8-aq)2(NO3)(H2O)]NO3 (5). As can be seen in Figure1E, the molecular structure of 5 shows some structural similarities with 4 and others described earlier (Table 4). As previously mentioned, each copper atom forms two fivemembered chelate rings with two 8-aq ligands inclined to one another by 9.36° and coordinated in the "head-to-tail" fashion distances, 2.937(7), 2.946(7) Å) hydrogen bonds involving coordinated nitrate and 8-aq molecules parallel to the bc plane. In fact, the coordinated NO_3^- anions connect adjacent infinite chains. Also, noncoordinated NO_3^- anions are inserted in the interchain spaces and join to adjacent chains by the establishment of N–H···O (N/O distance 3.01(1) Å) hydrogen- bonding interactions. Additionally, π–π stacking interactions (centroid-to-centroid distance Cg1···Cg2 = 3.677 Å) are found, between neighboring 8-aq rings connecting the infinite 1D chains (shown in Figure 6). Hydrogen-bonding and π–π stacking interactions stabilize the crystal structure and give rise to a 2D layered supramolecular network.

3.2.6. [Cd(8-aq)2 I2] (6). Complexes 1 and 6 are isostructural, and consequently, they exhibit similar structural features and self-assembled dimers in the solid state. Thus, complex 6 is described briefly. The asymmetric unit of 6 is shown in Figure 1F together with the atomic numbering scheme. As previously mentioned in 1, two 8-aq units are coordinated to the metal center atom in a nearly perpendicular fashion, as indicated by the cis N2–Cd(1)–N2i angle of 94.21(17)°, and the remaining sites are occupied by both I^- counteranions forming a distorted octahedral coordination environment. Moreover, the neutral complexes are held together by means of N–H···I (N/I distance 3.826(4) Å) hydrogen-bonding interactions to create R2 2(8) rings along the c direction axis. The infinite 1D chains generated by the N–H···I hydrogen bonds are interconnected by π–π antiparallel stacking interactions (Cg1···Cg1 = 3.562 Å and Cg1···Cg2 = 3.580 Å) (see Figure 7).

Figure 7.

Figure 8.

(Cu–N1, 2.027(6) Å, Cu–N2, 1.998(6) Å, Cu–N3, 2.023(6) Å, Cu–N4, 2.002(3) Å). The Cu–N(1) and Cu–N(2) bond distances in 4 and 5 are similar to those found in other compounds.39,40 In this case, the Cl atom is replaced by a NO_3^- anion (Cu–O3A, 2.616(4) Å) in the axial position, which forms the distorted octahedral environment around the Cu atom. The structural units can be further expanded into 2D layers by hydrogen-bonding interactions. Mononuclear complexes are linked together by means of N–H···O (N/O

3.3. CSD Search. There are 42 examples of transition-metal complexes of the 8-aq ligand in the Cambridge Structural Database (CSD), where most of them have Zn, Cd, Fe, Ni, Mn, and Co as metal centers. By comparison of the structures 1–6 reported herein and the crystal structures present in CSD search, the following considerations arise. First, as seen in Table 4, the average M–N bond lengths for 1–6 are close to the reported values for complexes of manganese, copper, and cadmium. In addition, M–N bond lengths (Namino and Nring belonging to 8-aq) for the Zn(II), Cd(II), Hg(II), Mn(II), and Fe(II) complexes are longer than those for the Co(II), Ni(II), and Cu(II) complexes. This difference in bond length may be caused by the electron configuration of the metal ion. Second, the structures reported herein illustrate that the accompanying anions play a vital role in the geometry and crystal packing of the M(8-aq)2 complexes. The quinoline system favors synergic back-bonding; therefore, its presence as a basal ligand would be energetically more favorable than as an apical ligand to favor the π-acceptor mechanism.31 Consequently, in most 8-aq complexes found in the CSD (similar to 2, 4, and 5), the ligand lies in a basal plane and is almost coplanar with the metal center. However, in the presence of SCN^- and I^- anionic coligands, both 8-aq ligands are perpendicular to each other in the coordination environment around the Mn and Cd (compounds 1, 3, and 6). Among the reported structures with 8-aq, there are only four structures with a cis configuration and three of them contain SCN^- as accompanying anion. Also, by examining the Cd/8-aq complexes with various counteranions such as Cl^-, N_3^-, I^-, and SCN^-, it is clear the important role of anion size on the X-ray structure. Complexes involving Cl^- and N_3^- anions are 1D coordination polymers, wherein these anions act as a bridging ligands, while SCN^- and I^- anions coordinate to CdII ions as a monodentate terminal ligands (see Table 4). In the compounds reported in this work, the accompanying anions also cause some differences in the self-organization of the crystal structures. The presence of diverse hydrogen bonds, such as N–H···I for 1 and 6, N–H··· Br and N–H···O for 2, N–H···S for 3, N–H···Cl and O–H··· Cl for 4, and O–H···O and N–H···O for 5, leads to some differences in terms of space group, dimensionality, and crystal growth.

3.4. Theoretical Studies of Noncovalent Interactions. The theoretical study is devoted to analyze several aspects of the geometric features and crystal packing characteristics of complexes 1−6. In particular, we have first analyzed the interaction energies of the H-bonding interactions that are possible due to the cis arrangement and provoke the generation of infinite 1D chains in the solid state. Second, we have studied the π-stacking interactions of the 8-aq ligands that are observed in the solid state of all compounds (see Figures 2−7). Finally, we have analyzed the coordination of some model Cu(8-aq)2X2 complexes to one or two water molecules and how this affects the stability of the complex. In Figure 8, we show the H-bonding assemblies observed in the solid state of compounds1, 3, and 6. The cis configuration allows the generation of infinite 1D columns as a consequence of high spatial complementary of the NH2 acceptor and I donor groups, that is, double N−H···I hydrogen bonds in the isostructural compounds 1 and 6 and bifurcated NH2···S2 hydrogen bonds in 3. We have computed the interaction energies of several dimers retrieved from the X-ray structures at the BP86-D3/def2-TZVP level of theory, and the results are included in Figure 8. The isostructural compounds present similar interaction energies and H-bond distances (ΔE1 = −18.2 kcal/mol and ΔE3 = −16.9 kcal/mol for 1 and 3, respectively). In compound 2, the interaction energy is larger in absolute value, likely due to higher electron donor ability of S.
These large interaction energies are due to the strong acidity of the NH2 protons because of the coordination to the transition metal. We have further analyzed the complementarity in the self-assembled dimers and the acidity of the NH2 protons in compound 6 by computing the molecular electrostatic potential (MEP) surface (see Figure 9). It can be observed that the strongest positive electrostatic potential region (71 kcal/mol) corresponds to one of the hydrogen atoms of the NH2 group, which is the H atom that forms the H-bonding interaction. This very positive potential is a clear indication of the strong acidity of this H atom. The electrostatic potential at the other H atom is considerably lower (48 kcal/mol). In addition, the most negative electrostatic potential corresponds to the iodide ligands, and more precisely in the region of the iodine atom that is interacting with the N−H bond. Therefore, there is a strong complementarity in the self-assembly of these complexes, facilitating the formation of the 1D chain in the solid state. We have also analyzed the interaction energies of the stacking interactions that are common in all complexes reported herein (see Figures 2−6). They are gathered in Table 5 ranging from −17.0 to −11.1 kcal/mol. These very favorable interaction energies are related to the short distances and the large π-system provided by the 8-aq ligand. It should be mentioned that, in compounds 4 and 5, the stacking interaction is established between two positively charged moieties, [Cu(8- aq)(Cl)(H2O]+ and [Cu(8-aq)(NO3)(H2O]+respectively, and consequently, a strong electrostatic repulsion is expected. As a matter of fact, if the outer sphere counterion is not considered in the calculations, the π−π stacking interaction is strongly repulsive (values in parentheses in Table 5). Finally, we have studied the substitution of coordinated halide ligands by water molecules in a Cu(8-aq)2X2 model complex (see Scheme 2). As described above, the Cu complexes 4 and 5 have a Cu-coordinated water molecule and one counterion (chloride or nitrate) that is not directly coordinated to the metal center. Using the reaction mechanism shown in Scheme 2, we have analyzed the reaction energies for a progressive substitution of halide ligands by water molecules to rationalize this experimental observation. Interestingly, it can be observed that the substitution of the first halide ligand (ΔE4) is strongly favored energetically for chloride and bromide and disfavored for iodide. In contrast, the second substitution is not favorable for any halide. These findings are in good agreement with the experimental results, since, in complexes 4 and 5, only one coordinated water molecule

Figure 9.

Table 5.

4. CONCLUSION

The synthesis and X-ray characterization of several metal complexes of 8-aminoquinoline are reported to analyze the effect of both the metal ion (manganese/8-aq, copper/8-aq, and cadmium/8-aq) and the counterion (I−, Br−, SCN−, Cl−, and NO3 −). The structural versatility of these M/8-aq systems is rather remarkable and reflects the variability in metal coordination sphere, orientation of the organic ligand, and the ability of inorganic anions to bind to the metal center. These results clearly reveal the significant role of the metal center and accompanying anions in the compositions of compounds 1−6. More importantly, in these systems, non-covalent interactions (hydrogen bonds and π−π stacking interactions) between the 8-aq and inorganic ligands have a prominent influence on assembling the low-dimensional entities into high-dimensional supramolecular networks. In the theoretical study, the analysis of the contributions of the different noncovalent interactions to molecular recognition has been carried out by assigning discrete energy values to them. This may help to develop energy scoring functions for crystal engineering and drug design.

Scheme 2.

ASSOCIATED CONTENT

* Supporting Information

Crystallographic information files (CIF) of compounds 1−6 and Figure S1. This material is available free of charge via the Internet at http://pubs.acs.org. CCDC Nos. 1034175, 1034193, 1034183, 1020871, 1020872, and 1034168 contain the supplementary crystallographic data for this paper.

AUTHOR INFORMATION

Corresponding Authors

*E-mail: mirzaeesh@um.ac.ir (M.M.).

*E-mail: toni.frontera@uib.es (A.F.).

Notes

The authors declare no competing financial interest.

ACKNOWLEDGMENTS

M.M. gratefully acknowledges the financial support by the Ferdowsi University of Mashhad, Mashhad, Iran (Grant Nos. 23919/3, 23844/3, and 23920/3). This work was also supported by the MINECO of Spain (projects CTQ2011-27512/BQU, and CONSOLIDER INGENIO 2010 CSD2010-00065, FEDER funds), and the Direccio´ General de Recerca i Innovació del Govern Balear (project 23/2011, FEDER funds). P.B. thanks Gobierno de Espan˜a MINECO (project CTQ2011-23014), Severo Ochoa Excellence Accreditation 2014-2018 (SEV-2013-0319), and the ICIQ Foundation for funding. We also thank Eduardo C. Escudero-Ada´n for X-ray crystallographic data. We thank the CTI (UIB) for free allocation of computer time. We also thank Tulane University for support of the Tulane Crystallography Laboratory.

REFERENCES

(1) Lehn, J.-M. Supramolecular Chemistry: Concepts and Perspectives; VCH: Weinheim, 1995.

(2) Ikkala, O.; Brinke, G. Science 2002, 295, 2407−2409.

(3) Zhang, J. P.; Lin, Y. Y.; Zhang, W. X.; Chen, X. M. J. Am. Chem. Soc. 2005, 127, 14162−14163.

(4) Toh, N. L.; Nagarathinam, M.; Vittal, J. J. Angew. Chem., Int. Ed. 2005, 44, 2237−2241.

(5) Pakhmutova, E. V.; Malkov, A. E.; Mikhailova, T. B.; Fomina, I. G.; Sidorov, A. A.; Aleksandrov, G. G.; Golovaneva, I. F.; Novotortsev, V. M.; Ikorskii, V. N.; Nefedov, S. E.; Eremenko, I. L. Russ. Chem. Bull., Int. Ed. 2003, 52, 139−149.

(6) Eshtiagh-Hosseini, H.; Mirzaei, M.; Zarghami, S.; Bauza´, A.; Frontera, A.; Mague, J. T.; Habibi, M.; Shamsipur, M. CrystEngComm 2014, 16, 1359−1377.

(7) Hong, M. C.; Zhao, Y. J.; Su, W. P.; Cao, R.; Fujita, M.; Zhou, Z. Y.; Chan, A. S. C. J. Am. Chem. Soc. 2000, 122, 4819−4820.

(8) Ma, J. F.; Liu, J. F.; Yan, X.; Jia, H. Q.; Lin, Y. H. J. Chem. Soc., Dalton Trans. 2000, 2403−2407.

(9) Aakero¨y, C. B.; Champness, N. R.; Janiak, C. CrystEngComm 2010, 12, 22−43.

(10) Carlucci, L.; Ciani, G.; Proserpio, D. M.; Rizzato, S. Chem.□ Eur. J. 1999, 5, 237−243.

(11) Wu, H.-P.; Janiak, C.; Rheinwald, G.; Lang, H. J. Chem. Soc., Dalton Trans. 1999, 183−189.

(12) Sertphon, D.; Harding, D. J.; Harding, P.; Adams, H. Polyhedron 2011, 30, 2740−2745.

(13) Genre, C.; Jeanneau, E.; Bousseksou, A.; Luneau, D.; Borshch, S. A.; Matouzenko, G. S. Chem.□Eur. J. 2008, 14, 697−705.

(14) Khavasi, H. R.; Mir Mohammad Sadegh, B. Inorg. Chem. 2010, 49, 5356−5358.

(15) Jung, O.-S.; Park, S. H.; Kim, K. M.; Jang, H. G. Inorg. Chem. 1998, 37, 5781−5785.

(16) Withersby, M. A.; Blake, A. J.; Champness, N. R.; Cooke, P. A.; Hubberstey, P.; Li, W.-S.; Schroder, M. Inorg. Chem. 1999, 38, 2259− 2266.

(17) Blake, A. J.; Brooks, N. R.; Champness, N. R.; Cooke, P. A.; Deveson, A. M.; Fenske, D.; Hubberstey, P.; Schroder, M. J. Chem. Soc., Dalton Trans. 1999, 2103−2110.

(18) Saalfrank, R. W.; Bernt, I.; Chowdhry, M. M.; Hampel, F.; Vaughan, G. B. M. Chem.□Eur. J. 2001, 7, 2765−2769.

(19) Kim, Y.; Kim, S.-J.; Choi, S. H.; Han, J. H.; Nam, S. H.; Lee, J. H.; Kim, H. J.; Kim, C.; Kim, D. W.; Jang, H. G. Inorg. Chim. Acta 2006, 359, 2534−2542.

(20) Paira, M. K.; Dinda, J.; Lu, T.-H.; Paital, A. R.; Sinha, C. Polyhedron 2007, 26, 4131−4140.

(21) Baruah, A. M.; Karmakar, A.; Baruah, J. B. Inorg. Chim. Acta 2008, 361, 2777−2784.

(22) Xu, H.; Huang, L.-F.; Guo, L.-M.; Zhang, Y.-G.; Ren, X.-M.; Song, Y.; Xie, J. J. Lumin. 2008, 128, 1665−1672.

(23) Mirzaei, M.; Eshtiagh-Hosseini, H.; Mohammadi Abadeh, M.; Chahkandi, M.; Frontera, A.; Hassanpoor, A. CrystEngComm 2013, 15, 1404−1413.

(24) Ryu, J. Y.; Lee, J. Y.; Choi, S. H.; Hong, S. J.; Kim, C.; Kim, Y.; Kim, S.-J. Inorg. Chim. Acta 2005, 358, 3398−3406.
(25) Cheng, P.-S.; Marivel, S.; Zang, S.-Q.; Gao, G.-G.; Mak, T. C. W. Cryst. Growth Des. 2012, 12, 4519−4529.
(26) Yoo, S.-K.; Ryu, J. Y.; Lee, J. Y.; Kim, C.; Kim, S.-J.; Kim, Y. Dalton Trans. 2003, 1454−1456.
(27) Hong, S. J.; Ryu, J. Y.; Lee, J. Y.; Kim, C.; Kim, Y.; Kim, S.-J. Dalton Trans. 2004, 2697−2701.
(28) Xu, Q.-F.; Zhou, Q.-X.; Lu, J.-M.; Xia, X.-W.; Wang, L.-H.; Zhang, Y. Polyhedron 2007, 26, 4849−4859.
(29) Malassa, A.; Go¨rls, H.; Buchholz, A.; Plass, W.; Westerhausen, M. Z. Anorg. Allg. Chem. 2006, 632, 2355−2362.
(30) Kerr, M. C.; Preston, H. S.; Ammon, H. L.; Huheey, J. E.; Stewart, J. M. J. Coord. Chem. 1981, 11, 111−115.
(31) Niu, C.; Wan, X.; Zheng, X.; Zhang, H.; Wu, B.; Niu, Y.; Hou, H. J. Coord. Chem. 2008, 61, 1997−2007.
(32) Genre, C.; Matouzenko, G. S.; Jeanneau, E.; Luneau, D. New J. Chem. 2006, 30, 1669−1674.
(33) CrysAlisPro, Version 1.171.36.32; Agilent Technologies: Santa Clara, CA.
(34) Sheldrick, G. M. SHELXS97: Program for the Solution of Crystal Structures; University of Go¨ttingen: Go¨ttingen, Germany, 1997.
(35) Sheldrick, G. M. SHELXL97: Program for the Refinement of Crystal Structures; University of Go¨ttingen: Go¨ttingen, Germany, 1997.
(36) Ahlrichs, R.; Ba¨r, M.; Ha¨ser, M.; Horn, H.; Ko¨lmel, C. Chem. Phys. Lett. 1989, 162, 165−169.
(37) Boys, S. F.; Bernardi, F. Mol. Phys. 1970, 19, 553−566.
(38) Nakamoto, K. Infrared Raman Spectra of Inorganic Coordination Compounds, Part B, 5th ed.; Wiley: New York, 1997.
(39) Williams, R. M.; Wallwork, J. C. Acta Crystallogr. 1967, 23, 448−455.
(40) Solans, X.; Font-Altaba, M.; Izquierdo, M.; Casabo´, J. Acta Crystallogr. 1985, C41, 46−47.
(41) Baruah, A. M.; Karmakar, A.; Baruah, J. B. Open Inorg. Chem. J. 2008, 2, 62−68.
(42) Niu, C.; Wan, X.; Zheng, X.; Zhang, H.; Wu, B.; Niu, Y.; Hou, H. J. Coord. Chem. 2008, 61, 1997−2007.
(43) Xu, H.; Liu, G.-X.; Huang, R.-Y.; Zhao, S.-P.; Kong, X.-J. Chin. J. Struct. Chem. 2013, 32, 545−549.
(44) Baruah, A. M.; Sarma, R.; Baruah, J. B. Inorg. Chem. Commun. 2008, 11, 121−124.
(45) Min, K. S.; Weyhermu¨ller, T.; Wieghardt, K. Dalton Trans. 2004, 178−186.
(46) Setifi, F.; Milin, E.; Charles, C.; Thetiot, F.; Triki, S.; Gomez- Garcia, C. J. Inorg. Chem. 2014, 53, 97−104.

Scheme 1. Synthetic Route to Compounds 1−6 Studied in This Work

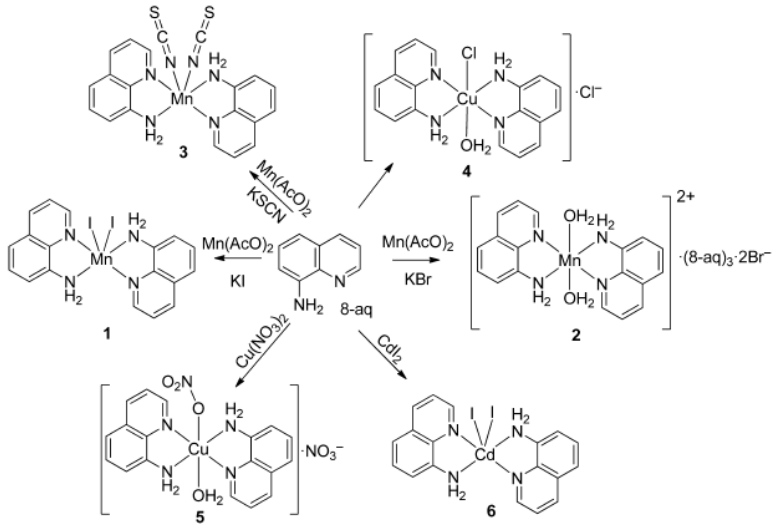

Table 1. Crystallographic Data for 1−6

	1	2	3	4	5	6
empirical formula	$C_{18}H_{16}I_2MnN_4$	$C_{45}H_{44}Br_2MnN_{10}O_2$	$C_{20}H_{16}MnN_6S_2$	$C_{18}H_{20}Cl_2CuN_4O_2$	$C_{18}H_{18}CuN_6O_7$	$C_{18}H_{16}CdI_2N_4$
formula weight (g mol^{-1})	597.09	971.66	459.45	458.57	493.92	654.55
temperature (K)	120 (2)	150 (2)	150 (2)	100(2)	100(2)	150 (2)
wavelength, λ (Å)	0.71073	0.71073	0.71073	0.71073	0.71073	0.71073
crystal system	monoclinic	monoclinic	orthorhombic	orthorhombic	monoclinic	monoclinic
space group	*I*2/*a*	$P2_1/c$	*Pbca*	*Pbca*	$P2_1/c$	*I*2/*a*
a (Å)	15.350 (3)	8.0468 (8)	8.4622 (7)	8.9805(7)	16.279(4)	15.5077 (11)
b (Å)	7.2871 (15)	10.9174 (11)	14.4899 (13)	12.9269(10)	14.820(3)	7.3367 (4)
c (Å)	16.305 (3)	23.914 (3)	32.093 (3)	32.531(2)	7.9174(15)	16.5357 (10)
α (deg)	90.00	90.00	90.00	90.00	90.00	90.00
β (deg)	95.95 (3)	96.6100 (13)	90.00	90.00	91.87(8)	95.9380 (16)
γ (deg)	90.00	90.00	90.00	90.00	90.00	90.00
volume ($Å^3$)	1814.0 (6)	2086.9 (4)	3935.2 (6)	3776.6(5)	1909.1(7)	1871.3 (2)
Z	4	2	8	8	4	4
D_c (mg m^{-3})	2.186	1.546	1.551	1.613	1.718	2.323
F(000)	1132	990	1880	1878	1012	1224
crystal size (mm^3)	0.42 × 0.38 × 0.20	0.15 × 0.13 × 0.10	0.15 × 0.14 × 0.12	0.20 × 0.15 × 0.06	0.30 × 0.10 × 0.003	0.22 × 0.14 × 0.13
θ range for data collection (deg)	2.50−25.00	2.50−28.00	2.50−29.20	1.25−25.67	1.25−26.47	2.50−29.10
index ranges	$-18 \le h \le 18$	$-10 \le h \le 10$	$-11 \le h \le 11$	$0 \le h \le 10$	$-20 \le h \le 20$	$-20 \le h \le 21$
	$-8 \le k \le 8$	$-14 \le k \le 14$	$-19 \le k \le 19$	$0 \le k \le 15$	$0 \le k \le 18$	$-10 \le k \le 10$
	$-19 \le l \le 1$	$-31 \le l \le 30$	$-43 \le l \le 44$	$0 \le l \le 39$	$0 \le l \le 9$	$-22 \le l \le 22$
reflections collected	4634	5150	5322	3521	5304	2459
refinement method	full-matrix least-squares on F^2	full-matrix least-squares on F^2	full-matrix least-squares on F^2	full-matrix least-squares on F^2	full-matrix least-squares on F^2	full-matrix least-squares on F^2
R_1, $wR_2[I > 2\sigma(I)]$	R_1 = 0.0390, wR_2 = 0.0993	R_1 = 0.0453, wR_2 = 0.1014	R_1 = 0.0360, wR_2 = 0.0835	R_1 = 0.0674, wR_2 = 0.1163	R_1 = 0.0669, wR_2 = 0.1795	R_1 = 0.0326, wR_2 = 0.0876
R_1, wR_2 (all data)	R_1 = 0.0438, wR_2 = 0.1018	R_1 = 0.0736, wR_2 = 0.11157	R_1 = 0.0510, wR_2 = 0.0936	R_1 = 0.1257, wR_2 = 0.1278	R_1 = 0.0886, wR_2 = 0.1917	R_1 = 0.0338, wR_2 = 0.0885
goodness-of-fit on F^2	1.08	1.022	1.03	1.158	1.085	1.06
largest differences peak and hole (e $Å^{-3}$)	1.99 and −2.26	0.868 and −1.048	0.39 and −0.26	0.466 and −0.586	0.903 and −0.904	2.86 and−0.66

Table 1. Christallographic data for 1-6

Table 2. Selected bond lenghths (A) and angles (deg) for 1-6.

		1	
Mn1–N1	2.318(5)	$N2^{i}$–Mn1–N1	95.36(16)
Mn1–N2	2.231(4)	N2–Mn1–I1	96.40(12)
Mn1–I1	2.9125(10)	N1–Mn1–I1	170.64(11)
N2–Mn1–N1	74.31(16)	$N1^{i}$–Mn1–I1	84.93(12)
$N2–Mn1–N2^{i}$	164.7(3)		
		2	
Mn1–N1	2.244(3)	$N2–Mn1–N2^{i}$	180.0
Mn1–N2	2.241(2)	O1–Mn1–N2	89.5(1)
Mn1–O1	2.216(3)	O1–Mn1–N1	93.4(1)
		3	
Mn1–N1	2.2572(15)	N3–Mn1–N4	73.33(5)
Mn1–N2	2.2977(15)	N5–Mn1–N3	94.60(6)
Mn1–N3	2.2557(15)	N6–Mn1–N1	95.67(6)
Mn1–N4	2.3062(15)	N5–Mn1–N1	99.85(6)
Mn1–N5	2.1870(17)	N6–Mn1–N5	86.85(6)
Mn1–N6	2.1847(18)	N6–Mn1–N3	100.84(6)
N3–Mn1–N2	90.28(5)	C19–N5–Mn1	161.47(15)
N1–Mn1–N2	73.66(5)	C20–N6–Mn1	172.90(17)
		4	
Cu1–N1	1.989(5)	N1–Cu1–N3	175.0(2)
Cu1–N2	2.020(5)	N4–Cu1–N3	84.1(2)
Cu1–N3	2.000(5)	N1–Cu1–N4	96.5(2)
Cu1–N4	1.999(5)	N4–Cu1–N2	178.0(2)
Cu1–O1	2.044(12)	N3–Cu1–N2	95.3(2)
Cl–Cu1–O1	171.7(1)		
		5	
Cu1–N1	2.027(6)	N4–Cu1–N3	84.2(2)
Cu1–N2	1.998(6)	N2–Cu1–N1	83.0(2)
Cu1–N3	2.023(6)	N4–Cu1–N1	97.3(2)
Cu1–N4	2.007(6)	N3–Cu1–N1	172.0(2)
Cu1–O3A	2.616(4)	N2–Cu1–O1	96.4(2)
Cu1–O1	2.323(4)	N4–Cu1–O1	87.4(2)
N2–Cu1–N4	176.1(2)	N3–Cu1–O1	93.5(2)
N2–Cu1–N3	94.9(2)	N1–Cu1–O1	94.4(2)
		6	
I1–Cd1	2.9225(4)	N1–Cd1–N2	71.11(11)
Cd1–N1	2.341(3)	$N2^{i}$–Cd1–N2	94.21(17)
Cd1–N2	2.441(3)	N1–Cd1–I1	97.10(8)
$N1^{i}$–Cd1–N1	159.70(16)	$I1–Cd1–I1^{i}$	98.281(17)

[a]Symmetry codes:(i) $-x + 3/2, y, -z + 1$ for **1**, (i) $-x + 2, -y + 2, -z + 1$ for **2**, (i) $-x + 1/2, y, -z + 1$ for **6**.

Table 3. Some of the Hydrogen-bonding Interactions present in 1-6.

D−H···A	d(D−H)/Å	D(H−A)/Å	d(D−A)/Å	D−H−A/deg
		1		
C3−H3···I1	0.950	3.231	4.0605(5)	147.63
		2		
N4−H4A···O1	0.91	2.24	3.155(4)	174
N4−H4B···Br1^{iii}	0.91	2.46	3.333(3)	161
N2−H2B···Br1^{v}	0.91	2.57	3.440(3)	160
N2−H2A···Br1^{iii}	0.91	2.46	3.356(3)	166
O1−H1A···N6^{vi}	0.84	2.34	3.146(5)	159
		3		
N2−H2A···S1^{i}	0.91	2.71	3.5303(16)	151
N2−H2B···S2^{i}	0.91	2.53	3.4250(16)	167
N4−H4A···S1^{ii}	0.91	2.63	3.5163(16)	164
N4−H4B···S2^{iii}	0.91	2.60	3.3121(16)	136
C10−H10···S2^{i}	0.95	2.94	3.827(2)	156
C11−H11···S2^{iv}	0.95	2.99	3.7489(19)	138
		4		
O1−H2O···Cl1	0.890	2.380	3.233(4)	161
O1−H1O···Cl1B	0.890	2.265	3.154(4)	176
O1W−H1W···Cl1B	0.891	2.241	3.129(4)	174
N1−H1A···Cl1	0.921	2.366	3.285(5)	176
		5		
N2−H2A···O1	0.920	2.035	2.937(7)	170
N2−H2B···O1	0.920	2.049	2.946(7)	162
N4−H4B···O2B	0.921	2.170	3.030(1)	157
		6		
C7−H7···I^{iv}	0.950	3.270	4.114(4)	149

[a]Symmetry codes:(iii) $x, y + 1, z$; (iv) $-x + 2, -y + 1, -z + 1$; (v) $-x + 1, -y + 1, -z + 1$; (vi) $x + 1, y + 1, z$ for **2**, (i) $-x + 3/2, y - 1/2, z$; (ii) $x - 1, y, z$; (iii) $-x + 1/2, y - 1/2, z$; (iv) $x + 1/2, -y + 1/2, -z + 1$ for **3**, (iv) $x - 1/2, -y + 2, z$ for **6**.

Figure 1. Molecular structure of compounds 1-6 with the atom numbering scheme.

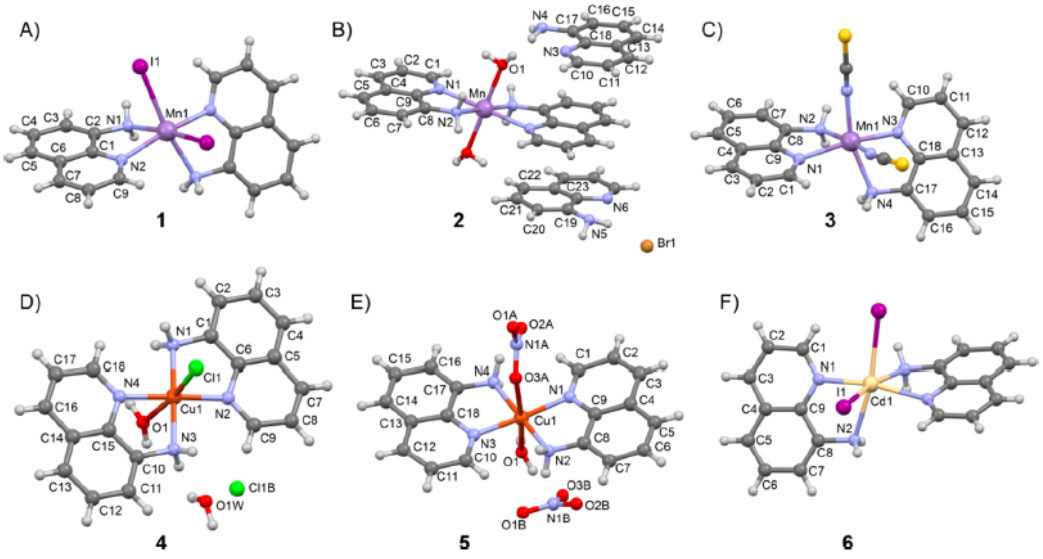

Figure 2. Crystal packing of compound 1 with indication of the hydrogen-bonding (A) and pi-pi stacking (B) dimers.

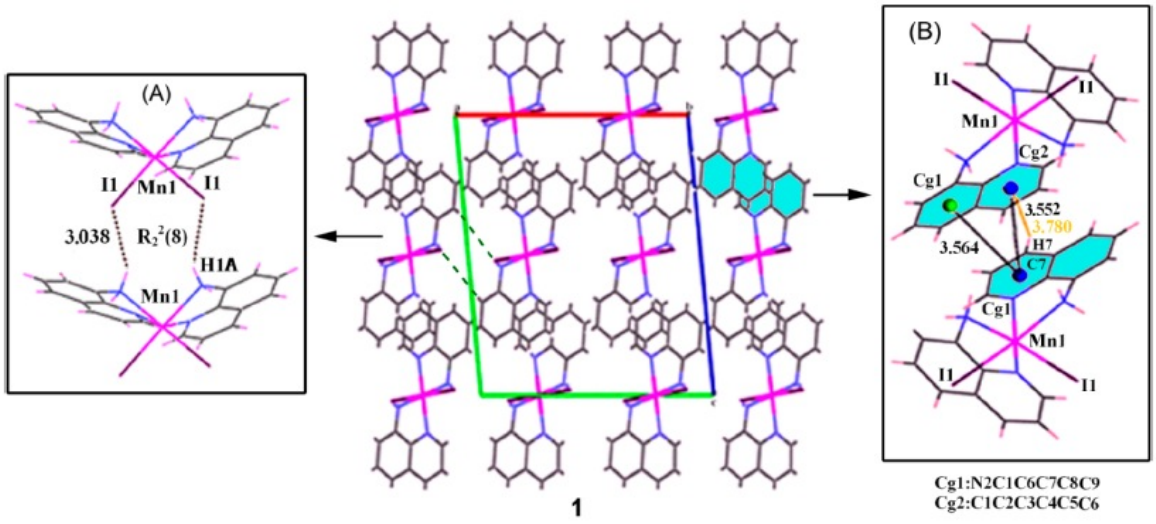

Figure 3. (A) crystal packaging of compound 2. (B) Detail of the pi-pi stacking between coordinated and uncoordinated ligands. Distances in A and angles in degrees.

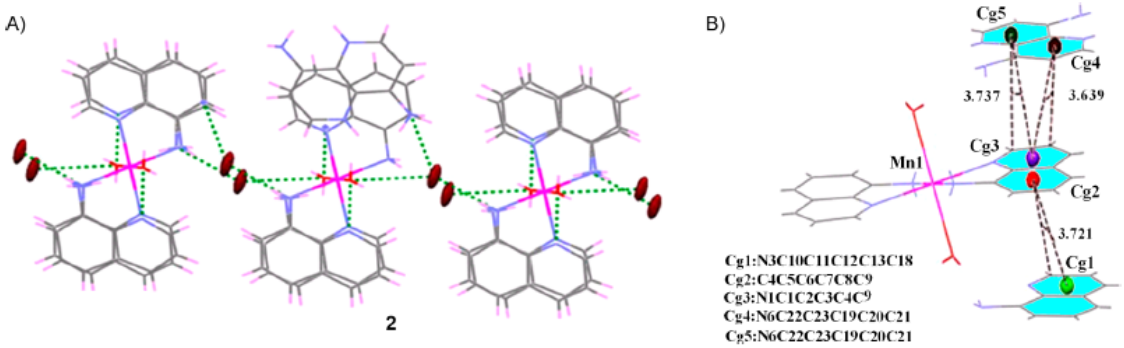

Figure 4. Crystal packaging of compound 3 with indication of the H-bonds (A) and the pi-stacking interactions (B). Distances in A.

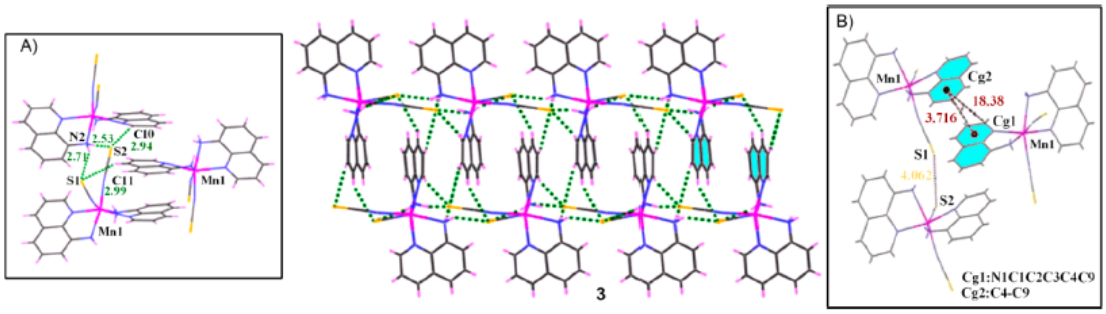

Figure 5. Crystal packing of compound 4 with indication of pi-stacking (A) and H-bonding (C) dimers. Distances in A.

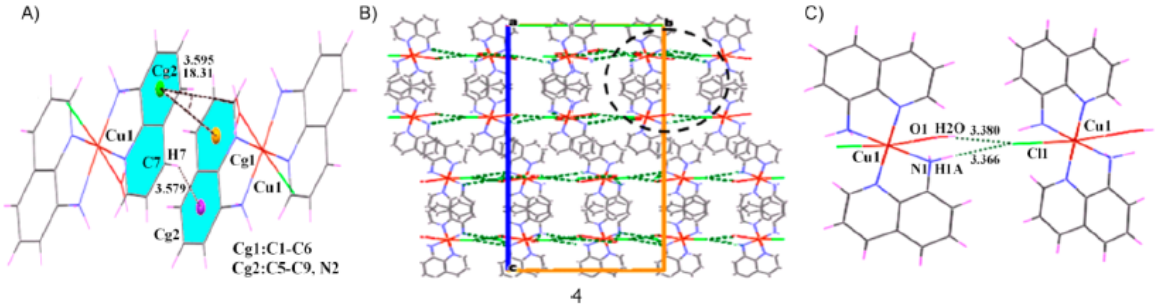

Table 4. Comparison of the Bond Distances (A) within some 8-aq Complexes.

compounds[a]	M–N_{amino}	M–N_{ring}	ref
1	2.319	2.230	this work
2	2.242	2.247	this work
3	2.298	2.257	this work
4	1.989, 2.000	2.000, 2.020	this work
5	1.998, 2.007	2.023, 2.027	this work
6	2.441	2.341	this work
$[Mn_3(2\text{-}NO_2\text{-}C_6H_4COO)_6(8\text{-aq})_2]$	2.26	2.24	41
$[[Mn_3(3\text{-}CH_3\text{-}C_6H_4COO)_6(8\text{-aq})_2]\cdot$NPD	2.25	2.28	41
$[Mn_2(2\text{-}NO_2\text{-}C_6H_4COO)_4(8\text{-aq})_2\ (H_2O)_2]$	2.24	2.23	41
$[Cu(NO_3)_2(8\text{-aqCl}_2)]$	2.00	1.96	40
$[Cd(8\text{-aq})(N_3)_2]_n$	2.358	2.317	19
$[Cd(8\text{-aq})_2SCN_2]$	2.62	2.39	21
$[Cd_2(\mu\text{-Cl})_4(8\text{-aq})_2]_n$	2.337	2.311	42
$[Zn(8\text{-aq})_2(SCN)_2]$	2.027, 2.023	1.998, 2.002	43
$[Zn(8\text{-aq})_2(H_2O)_2](NO_3)_2$	2.095	2.133	19
$[Zn(8\text{-aq})_2(BZ)]^+BZ$	2.19	2.10	44
$[Hg(8\text{-aq})Br_2]$	2.42	2.38	22
$[Hg_5(8\text{-aq})_2I_{10}]_n$	2.42	2.29	22
$[Co_2(NCS)_2(AP)_2(8\text{-aq})]$	2.07	1.89	45
$[Co_2(\mu_2\eta^2\text{-L})_2(\mu\text{-OOCCMe}_3)(L)(OOCCMe_3)_3]$	1.910	1.985	5
$[Ni(hfac)_2(8\text{-aq})]$	2.06	2.07	12
$[Fe(8\text{-aq})_2(4,4'\text{-bpy})](ClO_4)_2\cdot$2EtOH	2.07	1.96	32
$[Fe\ (\mu\text{-cyano})_2(8\text{-aq})_2\ (cyano)_2Ni]_n$	2.160	2.131	46

[a]Abbreviations: NPD = 1,5-dihydroxynaphthalene, BZ = benzoate, 4,4′-bpy = 4,4′-bipyridyl, L = 8-amino-2,4-dimethylquinoline, AP = 2-(8-aminoquinolino)-4,6-di-*tert*-butylphenol, hfac = hexafluoroacetylacetonate.

Figure 6. Crystal packing of compound 5showing the H-bonds (A) and the pi-stacking interactions (B). Distances in A.

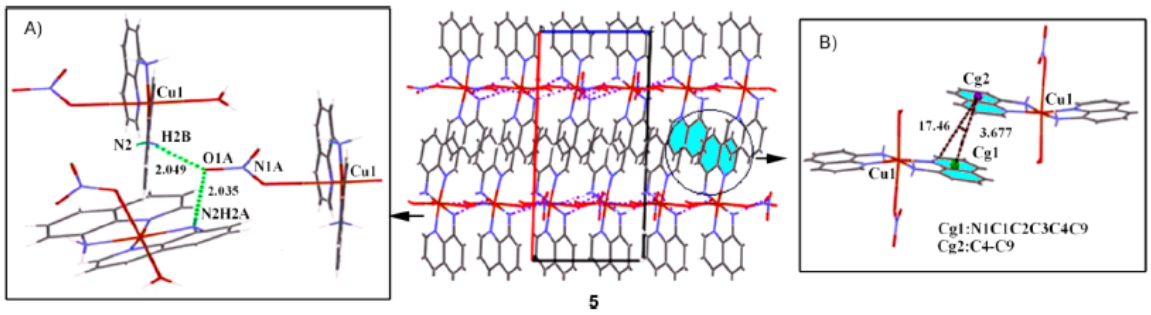

Figure 7. Crystal packing of compound 6 showing the H-bonds (A) and the pi-stacking interactions (B). Distances in A.

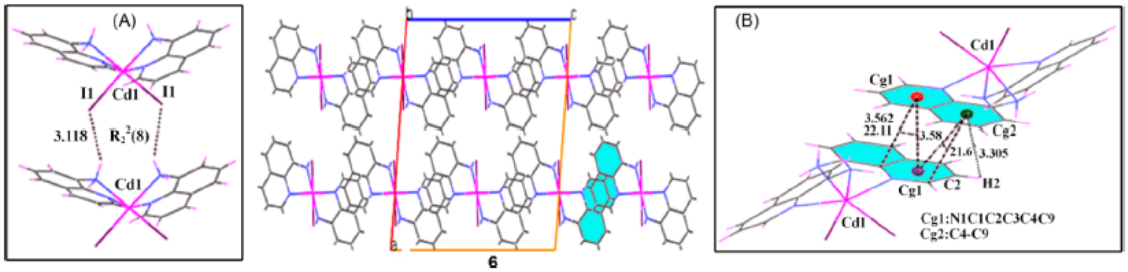

Figure 8. Hydrogen-bonding infinite 1D columns observed in the solid-state structures of 1, 3, and 6. Distances in A interaction energies of the dimers are also given.

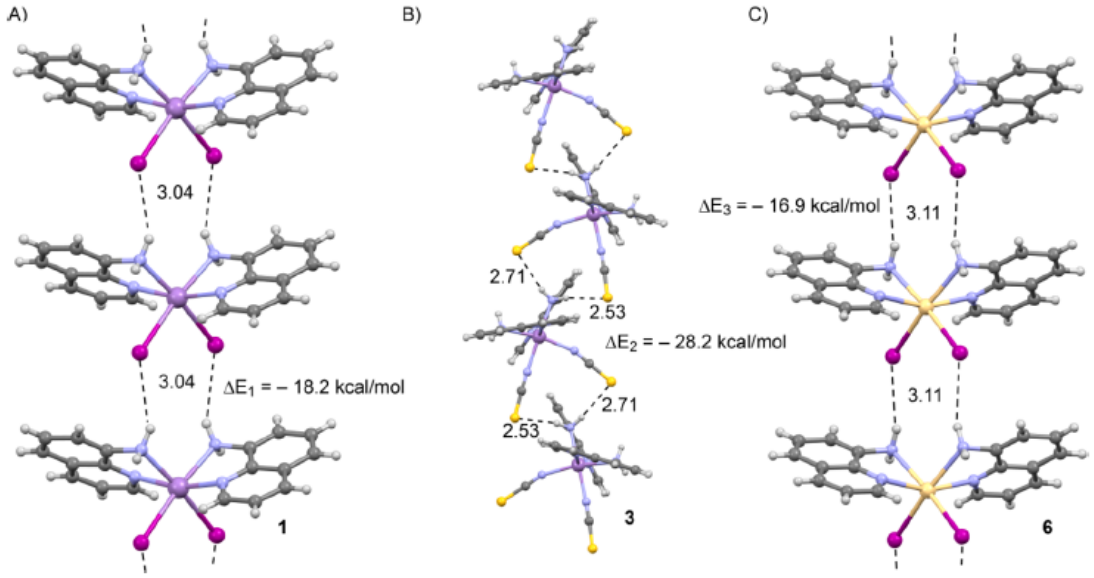

Table 5.

Table 5. π-Stacking Energies $\Delta E_{\pi-\pi}$ (kcal/mol) of and Centroid-to-Centroid ($Cg-Cg$) Distances (Å) for Compounds 1–6[a]

compound	$\Delta E_{\pi-\pi}$	$Cg-Cg$ distance	remark
1	−11.4	3.56	Figure 2B
2	−15.7	3.63	Figure 3B
3	−11.1	3.72	Figure 4B
4	−12.1 (+31.0)	3.59	Figure 5A
5	−17.0 (+33.5)	3.67	Figure 6B
6	−12.7	3.58	Figure 7B

[a]For the definitions of the centroids, see Figures 2–6.

Figure 9. MEP surface of complex 6 and the complementarity (highest positive potential region with the highest negative potential energy regions, blue and red, respectively).

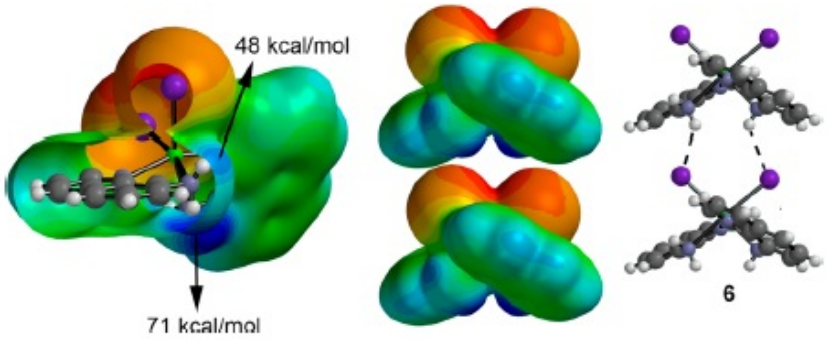

Scheme 2. Halide-water ligand substitution reactions.